ISBN: 978-3-95450-233-2 ISSN: 2673-5504 doi:10.18429/JACoW-SRF2021-SUPFDV009

THERMAL ANNEALING OF SPUTTERED Nb_3Sn AND V_3Si THIN FILMS FOR SUPERCONDUCTING RF CAVITIES*

K. Howard†, Z. Sun, M. U. Liepe, Cornell University, CLASSE, Ithaca, NY 14853, USA

Abstract

Nb_3Sn and V_3Si thin films are alternative material candidates for the next-generation of superconducting radio-frequency (SRF) cavities. However, past sputtered films suffer from stoichiometry and strain issues during deposition and post annealing. As such, we aim to explore the structural and chemical effects of thermal annealing, both in-situ and post-sputtering, on DC-sputtered Nb_3Sn and V_3Si with varying thickness on Nb or Cu substrates. We successfully enabled recrystallization of 100 nm thin Nb_3Sn films with stoichiometric and strain-free grains at 950 °C annealing. For 2 µm films, we observed removal of strain and slight increase in grain size with increasing temperature. A phase transformation from unstable to stable structure appeared on thick V_3Si samples, while we observed significant Sn loss in thick Nb_3Sn films at high temperature anneals. For films on Cu substrates, we observed similar Sn and Si loss during annealing likely due to Cu-Sn and Cu-Si phase generation and subsequent Sn and Si evaporation. These results encourage us to refine our process to obtain high quality films for SRF use.

INTRODUCTION

As niobium-based superconducting radio-frequency (SRF) cavities are reaching the theoretical limits, alternative materials are of great interest to continue the quest of increasing quality factors, accelerating gradients, and efficiency. A-15 superconductors Nb_3Sn and V_3Si are promising candidates for this role, used as thin films inside either Nb or Cu cavities [1, 2]. Both candidates have relatively high critical temperatures ($T_{c,Nb3Sn}$=18.3K and $T_{c,V3Si}$=17.1K), and Nb_3Sn is predicted to yield a superheating field of ~400 mT that doubles the Nb limit of ~200 mT [2-4]. These properties could allow cavity operation at an elevated temperature of 4.2K and the potential for increased accelerating gradients [5]. Due to their brittle nature and low thermal conductivity, Nb_3Sn and V_3Si are best suited for use as a thin film inside a host cavity with better thermal conductivity, such as Nb or Cu [2, 6, 7]. Here, we investigated Nb_3Sn and V_3Si films of different thickness on both Nb and Cu substrate to optimize the best conditions that overcome cracking while producing required stoichiometry and properties.

Sputtering that utilizes high-energy plasma to eject target materials is a promising technique for deposition of these films onto the substrates [1]. The film properties can be tailored via controlling the Ar plasma pressure, substrate temperature, sputtering voltage, sputtering current, and rate of deposition. In literature, sputtered Nb_3Sn films have been demonstrated on Nb and Cu surfaces either using direct a Nb_3Sn target or through annealing a sputtered Nb/Sn multilayer, and achieved T_c above 17 K [1, 4, 5, 8], while V_3Si has not yet been extensively studied for SRF use [6, 7]. One goal of this work is to optimize the sputtering capability of these alternative SRF materials at Cornell and compare our results with existing efforts in the SRF field.

Thermal annealing of the sputtered films, either in-situ or post deposition, is required to minimize the internal stress induced by the sputtering process and improve the stoichiometry and grain structures, which are critical to their critical temperature and cavity RF performance. However, during annealing of sputtered Nb_3Sn or Nb/Sn multilayers, the films suffer from issues such as the Sn loss, Cu incorporation into the film for Cu substrates, and lattice mismatch at the substrate-film boundary [1, 4, 8]. Thus, we aim to systematically investigate the effect of thermal annealing on the sputtered Nb_3Sn and V_3Si thin films in order to better understand these observed issues and design an optimal process for SRF use.

METHODS

In this study, Nb_3Sn and V_3Si thin films were deposited using a DC-sputtering system at the Cornell Center for Materials Research. These films varied in thickness, substrate, and heating in-situ. In the sputtering process, bulk Nb_3Sn and V_3Si targets were used, and all depositions were performed at 5 mTorr Ar pressure. The substrates were square-shape samples of Nb (1 cm x 1 cm x 3 mm) and Cu (1 cm x 1 cm x 2 mm). Before deposition, Nb substrates were electropolished and Cu substrates were chemically polished to ensure a smooth surface.

The sputtering parameters studied are the film material (Nb_3Sn vs. V_3Si), substrate material (Nb vs. Cu), deposition temperature (room temperature vs. 550 °C in-situ heating), and film thickness (100 nm, 300 nm, and 2 µm). After the sputtering process, films were annealed under different temperatures (600 °C - 950 °C) for 6 hours in a Lindberg high-vacuum (10^{-7} Torr) furnace. Structural and chemical analysis were conducted between anneals to characterize the films. These analysis methods included scanning electron microscope (SEM) to observe the grain structure and size, energy dispersive X-ray spectroscopy (EDS) to calculate the atomic composition, and X-ray diffraction (XRD) to gain insight about the crystal structure of the film and calculate the strain. In this analysis, the key features we are looking for are the quality of the film surfaces (smoothness, uniformity, grain shape/size), the stoichiometry of the films, and the existence and strain of Nb_3Sn and V_3Si diffraction planes.

* This work was supported by the U.S. National Science Foundation under Award PHY-1549132, the Center for Bright Beams. This work made use of the Cornell Center for Materials Research Shared Facilities which are supported through the NSF MRSEC program (DMR-1719875).
† khoward99@uchicago.edu

20th Int. Conf. on RF Superconductivity SRF2021, East Lansing, MI, USA JACoW Publishing
ISBN: 978-3-95450-233-2 ISSN: 2673-5504 doi:10.18429/JACoW-SRF2021-SUPFDV009

RESULTS

Surface Morphology and Grain Information

The changes to the surface morphology with increasing temperature give insight to the formation and structure of Nb_3Sn and V_3Si grains. In this section, SEM images of each sample are shown at an image width of 5 µm at different temperature points.

In the 100 nm Nb_3Sn sample on a Nb substrate, we observe the recrystallization of the film at 950 °C with a larger 300 nm grain size, shown in Fig. 1. This change occurs between 800 °C and 950 °C and represents the removal of strain in the film to form stoichiometric Nb_3Sn.

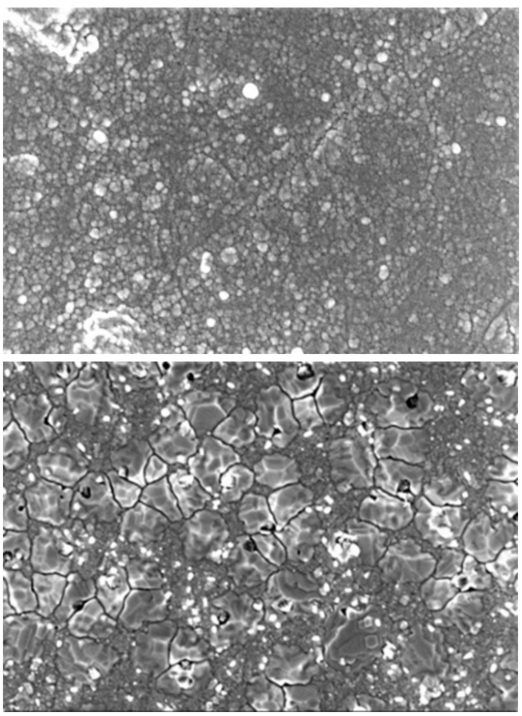

Figure 1: 100 nm Nb_3Sn on Nb SEM. (top) Initial 25 °C. (bottom) 950 °C. Image width: 5 µm.

For the 2 µm Nb_3Sn sample on a Nb substrate as shown in Fig. 2, triangular grains exist at all temperatures, and barely change with each anneal. We believe this signifies high in-plane stress on the thick film during deposition that was removed *in situ* by nucleating triangular small-sized grains.

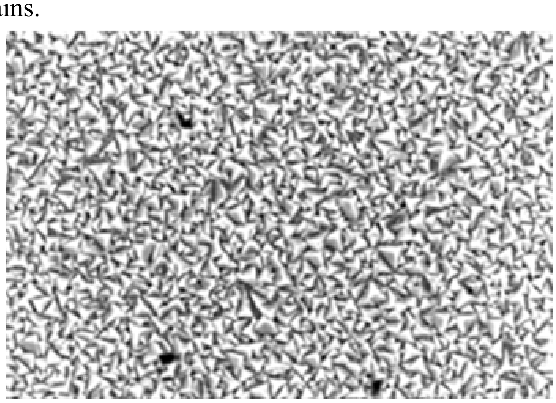

Figure 2: 2 µm Nb_3Sn on Nb. Initial ~400 °C. Image width: 5 µm.

In the 300 nm Nb_3Sn sample on a Cu substrate in Fig. 3, the grain structure changes dramatically due to the generation of Cu-Sn phases, starting with small, rounded grains collecting in finger-like formations and remelting into small angular grains collecting in regions of differing densities.

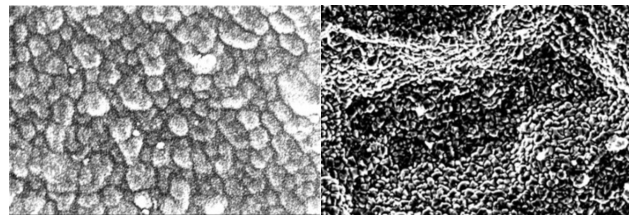

Figure 3: 300 nm Nb_3Sn on Cu SEM. (left) Initial 550 °C. (right) 950 °C. Image width: 5 µm.

For the 2 µm V_3Si sample on a Nb substrate in Fig. 4, large cracks begin to appear on the film after the first anneal at 600 °C, coinciding with a shift toward a more angular grain shape with increasing temperature.

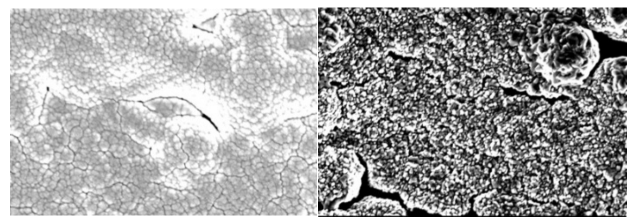

Figure 4: 2 µm V_3Si on Nb SEM. (left) Initial ~400 °C. (right) 950 °C. Image width: 5 µm.

The 300 nm V_3Si sample on a Cu substrate in Fig. 5 begins with a finger-like pattern after deposition and ends with small angular grains and large artifacts scattered across the surface after 950 °C anneal. These changes are all due to the generation of Cu-Si phases. Overall, there is a trend of grain angularization and pattern restructuring with increasing temperature.

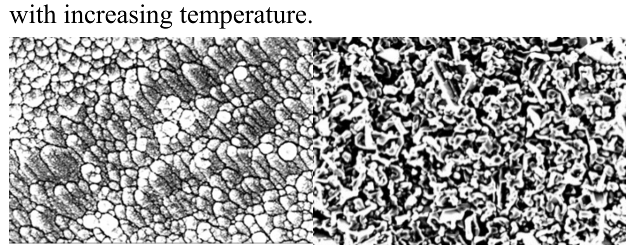

Figure 5: 300 nm V_3Si on Cu SEM. (left) Initial 550 °C. (right) 950 °C. Image width: 5 µm.

Atomic Composition

Measuring the atomic percentages through EDS is important to this study in order to understand whether we have obtained stoichiometric films. We performed EDS on the 2 µm and 300 nm samples and then calibrated the results with regard to the electron penetration depth in each material and the film thickness. This calibration allowed us to distinguish between measurements from the film and the substrate. The EDS results for these samples are shown in Table 1. For the Nb_3Sn samples, there are near-stoichiometric initial values of Sn and then significant Sn loss with increasing temperature. The 2 µm and 300 nm Nb_3Sn films behaved similarly for these measurements. For the V_3Si

ISBN: 978-3-95450-233-2 ISSN: 2673-5504 doi:10.18429/JACoW-SRF2021-SUPFDV009

samples, we observed near-stoichiometric final values of Si. The 2 µm sample has a constant Si concentration for all temperatures, whereas the 300 nm sample begins with high Si concentration and then drops to 20% after heating. Cu is evident in the 300 nm samples, but is not included in this ratio, which accounts for the extreme initial values in the 300 nm V_3Si sample. This phenomenon is due to the Cu inclusion at lower temperatures that is expelled either to the vacuum or back into the substrate above 700 °C based on the V-Si-Cu phase diagram.

Table 1: EDS Results

Sample	Sn or Si Atomic Ratio (%)		
	Initial	700 °C	950 °C
2 µm Nb_3Sn	21	13	2
300 nm Nb_3Sn	24	10	0
2 µm V_3Si	23	23	23
300 nm V_3Si	42	39	20

Lattice Structure

Using XRD is important for understanding how the structure of the crystal lattice changes with temperature. By identifying which peaks correspond to Nb_3Sn/V_3Si planes and tracking their positions at each temperature measurement, we can reveal the development of the lattice structure. The large peaks generally refer to the substrate material, so the small peaks must be analyzed for the relevant data. The raw XRD data for the 100 nm Nb_3Sn sample on a Nb substrate is shown in Fig. 6. In this sample, we observe Nb_3Sn peaks near the known powder diffraction peaks at 2θ = 33.6, 37.7, 41.5, 62.8, 65.6, 70.6, and 82.9 [9]. The detection of these peaks increases with temperature, which reflects the recrystallization observed in the SEM data.

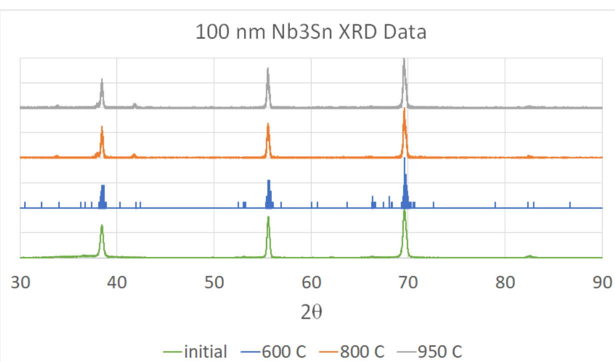

Figure 6: This XRD data shows the intensity versus 2θ for each temperature of the 100 nm Nb_3Sn film on a Nb substrate, starting with the initial measurement on the bottom and moving upward with increasing temperature.

In the 2 µm V_3Si sample on a Nb substrate, the film undergoes a transition from the unstable V_3Si structure to the stable structure between 800 °C and 950 °C. This is observed through the shifting of the 220 diffraction peak in Fig. 7. This transition shows how annealing contributes to the removal of the strain in a thick film. In the 300 nm film on a Cu substrate, we observe only the unstable phase at low temperatures and then both phases coexisting at and above 800 °C. The unstable to stable transition is not as dramatic here, but we still find annealing as a mechanism of strain removal for both samples.

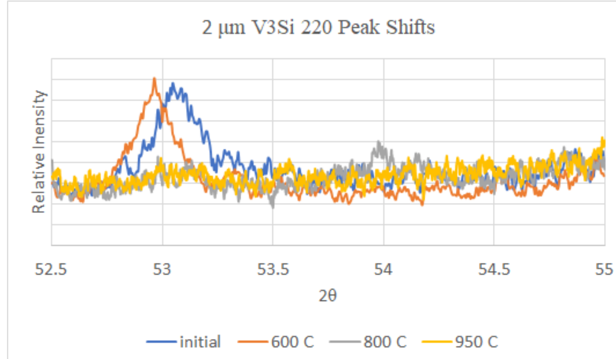

Figure 7: This graph shows the shifting of the 220 diffraction peak of the 2 µm V_3Si sample on a Nb substrate to increasing 2θ at high temperature, representing the shift from unstable to stable structure. By using an exponential smoothing method to reduce noise, the 950 °C peak at 54.5 is not shown.

In all samples, peaks corresponding to Nb_3Sn/V_3Si are found. However, there is an interesting discrepancy in the 2 µm and 300 nm Nb_3Sn films, as there is increased detection of Nb_3Sn peaks with increasing temperature, but the EDS data shows the complete loss of Sn by 950 °C. We also observed peaks unrelated to the substrates or intended films at low temperatures, which are believed to be from alternate Nb-Sn/V-Si phases or due to incorporation of Cu in the 300 nm films. Further exploration of the crystal structure and phase diagrams is required to resolve these issues.

CONCLUSION

In this study, we have demonstrated the capability of annealing sputtered thin films to produce successful Nb_3Sn and V_3Si surfaces that have potential for use inside SRF cavities. We observed that annealing is required to release the strain in the film and promote grain growth. For our Nb_3Sn samples, the best results are found on our recrystallized 100 nm film, where Nb_3Sn peaks emerged at 800 °C and large grains formed at 950 °C. This sample was also smooth and had minimal surface defects. The 2 µm and 300 nm films were not able to overcome this strain barrier and likely formed an amorphous Nb-Sn phase that led to near complete Sn loss during annealing. In addition, changes in the surface morphology are a sign of high initial strain. The emergence of Nb_3Sn peaks at high temperatures suggests that annealing promotes a small amount of the amorphous Nb-Sn phase into crystalline Nb_3Sn, but that the majority is removed through evaporation. For the V_3Si samples, we observed a transition in the grain shape to become more angular with increasing temperature as well as stoichiometric films at high temperature. Most interesting was the behavior of the film with respect to the unstable and stable phases of V_3Si. In the 2 µm film, there was a complete transition from unstable to stable at 800 °C along with con-

ISBN: 978-3-95450-233-2 ISSN: 2673-5504 doi:10.18429/JACoW-SRF2021-SUPFDV009

sistent stoichiometry. For the 300 nm film, there was excess Si upon deposition that was removed through a partial unstable to stable transition. Because we observe this transition and the proper stoichiometry at high temperature, we determine these are successful V_3Si films.

For the Cu substrate samples, there was Cu inclusion into the films leading to Cu-Sn and Cu-Si phases at low temperatures. These phases were removed at high temperatures, but there were still high concentrations of Cu in the films. The Cu impurities and Cu-related phases could adversely affect the SRF performance of Nb_3Sn/V_3Si films inside Cu cavities. In a future study, we would be interested in the use of an ultrathin buffer layer between the Cu and the superconducting layer to prevent this effect [10].

In our results, we observed a similar Sn loss as in previous studies [4]. We are interested in finding ways to prevent this loss such as depositing crystalline Nb-Sn phases or using a buffer during the annealing process. We would like to obtain the benefits of annealing such as recrystallization and strain removal while avoiding events such as Sn loss and cracking. Because the 100 nm Nb_3Sn film was successful, it would be important in a future study to further investigate films of similar thickness to optimize the grain growth and RF performance.

REFERENCES

[1] E. A. Ilyina *et al*, "Development of sputtered Nb_3Sn films on copper substrates for superconducting radiofrequency applications," *Supercond. Sci. Technol.*, vol. 32, no. 3, p. 035002, Jan. 2019. doi:10.1088/1361-6668/aaf61f

[2] S. Posen and D. L. Hall, "Nb_3Sn superconducting radiofrequency cavities: fabrication, results, properties, and prospects," *Supercond. Sci. Technol.,* vol. 30, no. 3, p. 033004, Jan. 2017. doi:10.1088/1361-6668/30/3/033004

[3] N. Valles and M. Liepe, "The Superheating Field of Niobium: Theory and Experiment," in *Proc. SRF2011*, Chicago, IL, USA, July 2011, paper TUIOA05, pp. 293-301.

[4] M. N. Sayeed, U. Pudasaini, C. Reece, G. Eremeev, & H. Elsayed-Ali, "Properties of Nb_3Sn films fabricated by magnetron sputtering from a single target," *Appl. Surf. Sci.,* vol. 541, pp. 148528, Mar. 2020. doi:10.1016/j.apsusc.2020.148528

[5] R. D. Porter *et al*., "Update on Nb_3Sn Progress at Cornell University", in *Proc. 9th Int. Particle Accelerator Conf. (IPAC'18)*, Vancouver, BC, Canada, Apr. 4, pp. 2479-2482. doi:10.18429/JACoW-IPAC2018-WEPMF050

[6] F.L. Estrin *et al*., "Using HiPIMS for V3Si Superconducting Thin Films," presented at 9th Int. Workshop on Thin Films and New Ideas for Pushing the Limits of RF Superconductivity, March 2021. https://indico.jlab.org/event/405/contributions/8111/

[7] S. M. Deambrosis *et al*., "The Progress on Nb_3Sn and V_3Si," in *Proc. SRF2007*, Peking Univ., Beijing, China, Oct. 14-18, 2007, paper WE203, pp. 392-399.

[8] M. N. Sayeed, U. Pudasaini, C. E. Reece, G. Eremeev, H. E. Elsayed-Ali, "Structural and Superconducting Properties of Nb_3Sn Films Grown by Multilayer Sequential Magnetron Sputtering," *J. Alloys Compd.* 2019, vol. 800, pp. 272–278, Sept. 2019. doi:10.1016/j.jallcom.2019.06.017

[9] A. Jain*, S. P. Ong*, G. Hautier, W. Chen, W. D. Richards, S. Dacek, S. Cholia, D. Gunter, D. Skinner, G. Ceder, K. A. Persson (*=equal contributions). "The Materials Project: A materials genome approach to accelerating materials innovation," *APL Mater.*, vol. 1, no. 1, p. 011002, 2013. doi:10.1063/1.4812323

[10] S. Fernandez *et al*., "Magnetron sputtered Nb3Sn and V3Si thin films on copper substrates for SRF application," presented at Nb3SnSRF'20, Nov. 2020. https://indico.classe.cornell.edu/event/1806/contributions/1491/.